J Fluoresc (2013) 23:1179–1195
DOI 10.1007/s10895-013-1249-z

ORIGINAL PAPER

Tuning the Solution Phase Photophysics of Two *De Novo* Designed Hydrogen Bond Sensitive 9-methyl-2,3,4,9-tetrahydro-1*H*-carbazol-1-one Derivatives

Sujay Ghosh · Amrit Krishna Mitra · Chandan Saha · Samita Basu

Received: 6 March 2013 / Accepted: 17 June 2013 / Published online: 7 July 2013

Abstract Two new fluorophores, 6,7-dimethoxy-9-methyl-2,3,4,9-tetrahydro-1H-carbazol-1-one (DMTCO) and 5-methyl-8,9-dihydro-5H-[1,3]dioxolo[4,5-b]carbazol-6(7H)-one (MDDCO), first of their kind, have been synthesized from the corresponding methoxy and methylenedioxy derivatives of 2,3,4,9-tetrahydro-1H-carbazol-1-one respectively. Comprehensive photophysical characterization of these compounds has been carried out in sixteen different homogeneous solvents and binary solvent mixtures. Both of these compounds are sensitive to solvent polarity, but the sensitivity is much higher in electronic excited state observed by steady-state and time-resolved fluorescence experiments than in ground state studied by UV–vis absorption spectroscopy. The fluorescence spectral shifts are linearly correlated with the empirical parameters of the protic solvents and also the quantitative influence of the empirical solvent parameters on the emission maxima of the compounds has been calculated. The change in dipole moment of the compounds in their excited state has been calculated from the shifts in corresponding emission maxima in pure solvents. A higher dipole moment change of both DMTCO and MDDCO in protic solvents is due to intermolecular hydrogen bonding which is further confirmed by the comparison of their behaviour in toluene-acetonitrile and toluene-methanol solvent mixtures. From structural features, MDDCO is more planar compared to DMTCO, which is reflected better in fluorescence quenching of the former with organic bases, N,N-dimethylaniline and N,N-diethylaniline. Laser flash photolysis experiments prove that the quenching interaction originates from photoinduced electron transfer from the bases to the compounds.

Keywords 9-methyl-2,3,4,9-tetrahydro-1H-carbazol-1-one · Fluorescent probe · Lippert-Mataga calculation · Hydrogen bond sensitivity · Fluorescence quenching · Photoinduced electron transfer · Laser flash photolysis

Introduction

For the last few decades, increasing interest in various research fields has been attracted by organic molecules containing quinine, pyrene, oxazine, cyanine, carbazole and skeletons of similar kind with high photoluminescence efficiencies in the form of advanced materials for electronic and photonic applications [1]. Thus it is crucial to synthesize novel fluorophores that are amenable to further chemical functionalization and modification, which in turn is essential to obtain materials with tunable optoelectronic properties. Small-molecule fluorescent probes also represent an essential facet of chemical biology. Although numerous fluorophores are known, the quest for newer ones is still on as these molecules are indispensable tools for chemical biology, being ubiquitous as biomolecular labels, enzyme substrates, environmental indicators and cellular staining agents. Hence, it is an important challenge to create molecules with desired optical properties which lies in achieving an well-defined architecture while maintaining adequate electron density throughout the molecule. At times, a slight variation like acetylation, alkylation etc. in a known fluorophore framework can bring about a new dimension for exploration. This is because choosing a suitably functionalized probe to visualize a biochemical or biological process can be

Sujay Ghosh and Amrit Krishna Mitra are Equal Contributors.

S. Ghosh · S. Basu (✉)
Chemical Sciences Division, Saha Institute of Nuclear Physics, Kolkata 700064, India
e-mail: samita.basu@saha.ac.in

A. K. Mitra · C. Saha
Department of Clinical and Experimental Pharmacology, School of Tropical Medicine, Kolkata 700073, India

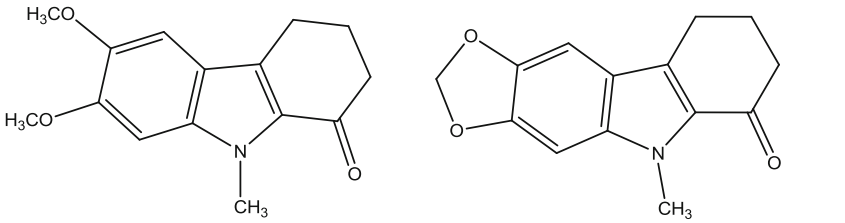

6,7-dimethoxy-9-methyl-2,3,4,9-tetrahydro-1*H*-carbazol-1-one (DMTCO)

5-methyl-8,9-dihydro-5*H*-[1,3]dioxolo[4,5-*b*]carbazol-6(7*H*)-one (MDDCO)

Fig. 1 Representative structures of DMTCO and MDDCO

beneficial of employing them as a biomarker after proper synthetic modulation.

Thus here we report the photo-physical aspects of two new derivatives 6,7-dimethoxy-9-methyl-2,3,4,9-tetrahydro-1H-carbazol-1-one (DMTCO) and 5-methyl-8,9-dihydro-5H-[1,3] dioxolo[4,5-b]carbazol-6(7H)-one (MDDCO) as shown in Fig. 1. The aim of the present work is mainly twofold, in which firstly, we endeavour to explore the solution phase photophysics of two fluorophores both in homogeneous and heterogeneous media. The second goal of the work is to study their photoinduced electron transfer interaction with aromatic donor units. Such studies are an essential prerequisite to determine the possible usage of any new fluorophores [2–12] and often can bring some extraordinary observations [13].

2,3,4,9-tetrahydro-1H-carbazol-1-one is an important synthetic precursor of carbazole nucleus. Carbazole alkaloids possess interesting biological properties, which include antitumor, psychotropic, anti-inflammatory, antihistaminic, antibiotic, and antioxidative activities [14, 15]. Literature survey reveals several reports based on the photophysical response of carbazole derivatives but no such extensive study has been performed on the 2,3,4,9-tetrahydro-1H-carbazol-1-one derivatives. During our project so far, we have witnessed 2,3,4,9-tetrahydro-1H-carbazol-1-one moiety when attached with electron donating substituents emits fluorescence. Our previous communications [16–18] reported the solvent response of the methoxy and methylenedioxy derivatives of 2,3,4,9-tetrahydro-1H-carbazol-1-one (Fig. 2).

Here we have synthesised DMTCO and MDDCO by transforming the NH functionality (marked in Fig. 2) to N-CH3 unit via simple chemical processes outlined in scheme 1.

Experimental Section

IR and NMR Spectroscopy

Melting points were determined in Digital Auto melting point apparatus (Scientific International). Reagent-grade chemicals were purchased from Merck India and used without further purification. All reaction mixtures and column eluents were monitored by TLC using commercial aluminum TLC plates (Merck Kieselgel 60 F254). IR spectra were recorded in KBr discs on Schimadzu FTIR- 8,300 and ^{1}H NMR and ^{13}C NMR spectra were recorded on Bruker AV 500 in DMSO-d_6 with tetramethylsilane as an internal standard. Data are reported as follows: chemical shift in ppm (δ), multiplicity (s = singlet, d = doublet, t = triplet, q = quartet, and m = multiplet), coupling constant (Hz). Results of APT (attached proton test) — ^{13}C NMR experiments are shown in parentheses where (+) denotes CH_3 or CH and (−) denotes CH_2 or C. High resolution mass spectra (HRMS) were performed on Qtof Micro YA263.

UV–vis and Fluorescence Spectroscopy

UV Spectroscopic grade Benzene (Bz), Toluene (Tol), 1,4-dioxane (DOX), Ethyl Acetate (EtAc), Tetrahydrofuran (THF), Acetonitrile (ACN), Dimethylformamide (DMF), Dimethylsulphoxide (DMSO), Water (HOH), Ethanol (EtOH), Methanol (MeOH) and Butanol (BuOH) have been purchased from Spectrochem Pvt. Ltd. and used as such. AR grade Hexanol (HxOH), Octanol (OcOH), Decanol (DcOH) and Dodecanol (DdOH) have been purchased from Loba Chemie Pvt. Ltd and used after proper distillation. The solvents have additionally been checked using steady- state and time-resolved fluorescence for lack of fluorescent impurities in the wavelength ranges of interest. Physical properties and empirical parameters of the solvents have been listed in Table 1. Anthracene has been purchased from Sigma-Aldrich and was used after proper recrystallization. Water from Milipore water purification system has been used. All experiments have been carried out using quartz cuvettes of 1 cm^2 cross-sections purchased from Hellma Analytics. No degradation of the compounds has been observed throughout the experimental period.

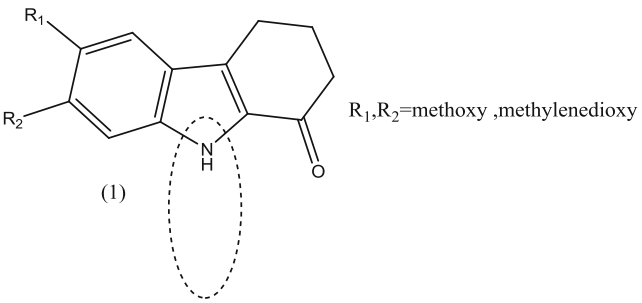

Fig. 2 Representative structures of methoxy and methylenedioxy derivatives of 2,3,4,9-tetrahydro-1H-carbazol-1-one

Scheme 1 Synthesis of DMTCO and MDDCO

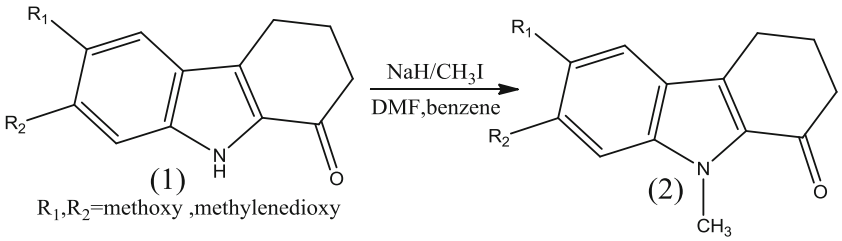

Jasco V-650 spectrophotometer and Horiba Jobin-Yvon Fluoromax-3 have been used for absorbance and fluorescence measurements respectively. Fluorescence lifetimes have been measured using a time-correlated single-photon-counting (TCSPC) spectrophotometer (Horiba Jobin-Yvon Single Photon Counting Controller Fluorohub). The sample has been excited at 340 nm using LED. The calculations have been performed using deconvolution technique, which is based upon a convolution integral, using the software supplied by Horiba Jobin-Yvon.

Nanosecond laser flash photolysis set-up from Applied Photophysics was used for the measurement of transient absorption spectra. The sample was excited at 355 nm using Nd-YAG laser (Lab series, Model Lab 150, Spectra Physics). Full width half-maximum of the exciting laser was 8 ns. Transient species in solution were monitored through absorption of light from a pulsed xenon lamp (150 W) at right angle to the laser beam. The wavelength from the probe beam was dispersed with a monochromator and detected with R928 photomultiplier detector. The photomultiplier output was fed into

Table 1 Physical properties and empirical parameters of solvents

Solvents	Dielectric Constant	Refractive Index	π^{*} [a]	α [b]	β [c]	$E_T(30)$ [d]
HOH	78.54	1.333	1.09	1.17	0.47	63.1
MeOH	32.6	1.326	0.6	0.98	0.66	55.4
EtOH	22.4	1.359	0.54	0.86	0.75	51.9
BuOH	18.2	1.397	0.47	0.84	0.84	49.7
HxOH	13.3	1.418	0.4	0.8	0.84	48.8
OcOH	10.3	1.429	0.4	0.77	0.81	48.1
DcOH	8.1	1.437	0.45	0.7	0.82	47.7
DdOH	6.5	1.442	–	–	–	47.5
Bz	2.28	1.498	0.59	0	0.1	34.3
Tol	2.38	1.494	0.54	0	0.11	33.9
DOX	2.21	1.42	0.55	0	0.37	36
EtAc	6.02	1.37	0.45	0	0.45	38.1
THF	7.6	1.404	0.51	0	0.54	37.4
ACN	37.5	1.342	0.75	0.19	0.31	45.6
DMF	36.7	1.427	0.88	0	0.69	43.2
DMSO	46.6	1.476	1	0	0.76	45.1

[a] π^{*} is the polarity or polarizability effects of the solvent

[b] α is the hydrogen bond donor (HBD) acidity of the solvent

[c] β is the hydrogen bond acceptor (HBA) basicity of the solvent

[d] $E_T(30)$ is the Dimroth-Reichardt empirical polarity parameter of the solvent

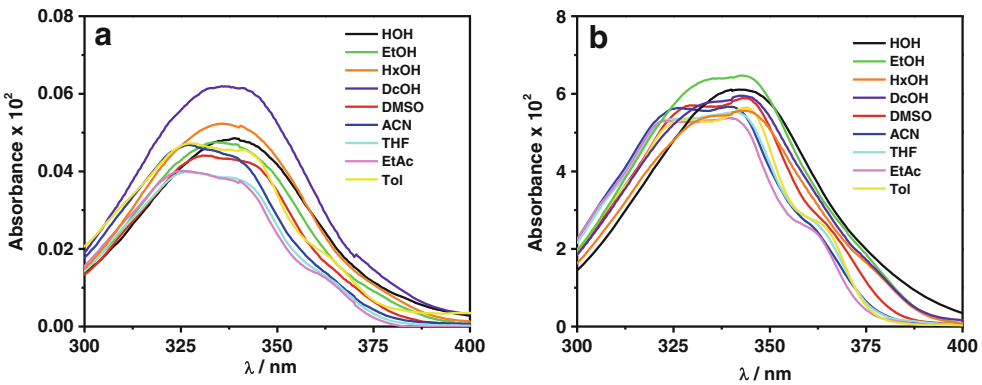

Fig. 3 Absorption spectra of **a** DMTCO and **b** MDDCO in nine different solvents. Concentrations of the compounds are 1×10^{-6} M during the experiment

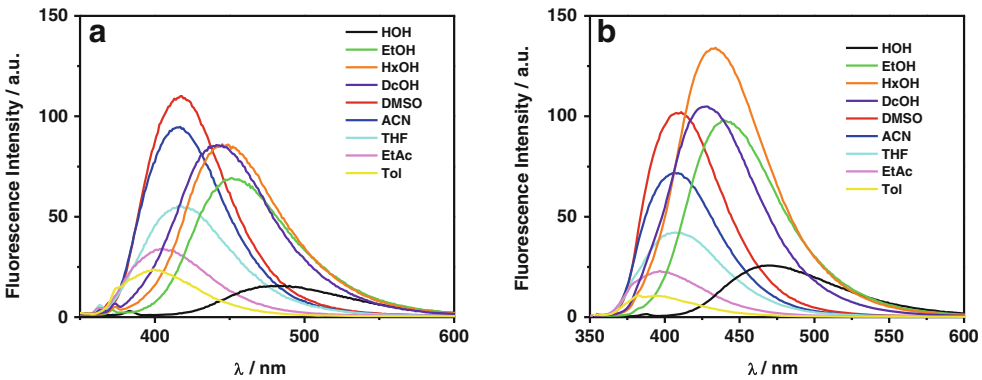

Fig. 4 Fluorescence emission spectra of **a** DMTCO and **b** MDDCO in nine different solvents after excitation at their respective absorption maxima. Concentrations of the compounds are 1×10^{-6} M during the experiment

a 600 MHz, 4 Gs/s, DSO8064A Agilent Infiniium oscilloscope, and the data were transferred to !Laser software running in an Iyonix range of ARM-based RISC OS computer. The samples were de-aerated for 20 min by passing pure argon gas prior to each experiment.

Data Analysis

All the data have been analysed, fitted and plotted by the software Origin® 8.0 Pro. Absorbance and Steady-state fluorescence measurements have been used to calculate the quantum yields of both DMTCO and MDDCO in pure solvents and to find out the maxima of the absorption and fluorescence spectra. Lippert-Mataga methods have been used to calculate the dipole moment change of the compounds in their electronic excited state in protic and aprotic solvents. Fluorescence maxima of the compounds in different solvents have been plotted with the empirical solvent parameters, e.g. empirical polarity paratemeter $E_T(30)$, H-bond donor acidity α, H-bond acceptor basicity β and polarizability π^* separately for protic and aprotic solvents. Kamlet-Taft solvatochromic comparison method has been used to quantify the individual contributions of different modes of solute-solvent interactions on the emission maxima of the fluorophores. Time-resolved fluorescence measurements have been performed to find out the fluorescence lifetimes of both the compounds in different solvents. Trends in non-radiative decay rates of the electronic excited states of the compounds in different solvents have been explained based on hydrogen bonding and intermolecular hydrogen bonding. 1,4-dioxane-water solvent mixture system has been used to show the similarity in photophysical behaviour of the fluorophores in pure solvents and binary solvent mixtures. Fluorescence emission of both DMTCO and MDDCO in toluene-acetonitrile and toluene-methanol solvent mixtures has been compared to establish the hydrogen bonding ability of both fluorophores.

Table 2 Absorption and emission maxima of DMTCO and MDDCO in sixteen different solvents

Solvents	DMTCO		MDDCO	
	Absorption Maxima	Fluorescence Maxima	Absorption Maxima	Fluorescence Maxima
DMSO	332	418	342	410
ACN	327	415	340	408
DMF	329	412	342	404
THF	327	417	341	407
EtAc	326	405	340	397
DOX	327	404	342	399
Bz	342	402	343	395
HOH	339	482	342	470
MeOH	335	461	343	448
EtOH	334	451	343	440
BuOH	336	449	345	437
HxOH	336	446	343	433
OcOH	334	443	337	429
DcOH	336	441	343	427
DdOH	335	440	343	425

Table 3 Quantum yield of DMTCO and MDDCO (10^{-6} M) in different solvents. Anthracene has been taken as reference

Solvents	DMTCO	MDDCO
BZ	0.036	0.038
TOL	0.031	0.021
DOX	0.045	0.052
EtAc	0.048	0.044
THF	0.084	0.089
ACN	0.129	0.140
DMF	0.123	0.142
DMSO	0.150	0.199
HOH	0.034	0.075
MeOH	0.123	0.215
EtOH	0.118	0.235
BuOH	0.157	0.253
HxOH	0.143	0.314
OcOH	0.157	0.288
DcOH	0.144	0.242
DdOH	0.038	0.006

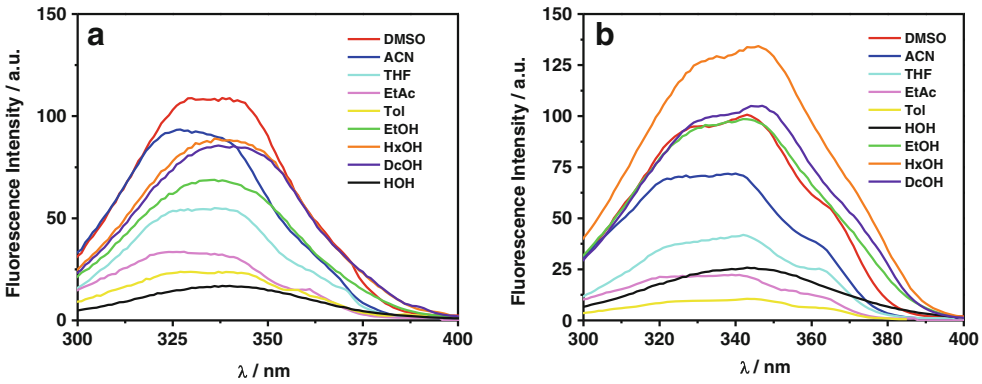

Fig. 5 Fluorescence excitation spectra of **a** DMTCO and **b** MDDCO in nine different solvents with respect to their corresponding emission maxima. Concentrations of the compounds are 1×10^{-6} M during the experiment

Steady state and lifetime fluorescence measurements have been used to determine the modes of interaction between both DMTCO and MDDCO with organic bases, N,N-dimethylaniline (DMA) and N,N-diethylaniline (DEA). That excited state interaction has been found to be due to photoinduced electron transfer (PET) from the organic bases to the compounds as measured by Laser Flash Photolysis experiments.

Synthetic Procedure

Methoxy and Methylenedioxy Derivatives of 2,3,4,9-tetrahydro-1H-carbazol-1-one (1)

For synthesis and spectral data, see reference 17.

Methoxy and Methylenedioxy Derivatives of 9-methyl-2,3,4,9-tetrahydro-1H-carbazol-1-one (2)

Derivatives of 2,3,4,9-tetrahydro-1H-carbazol-1-one (**1**, 20.0-mmol) were dissolved in DMF-benzene mixture (1:2, 30 mL) and allowed to cool at 0°C in ice bath. 55 % suspension of sodium hydride in mineral oil (1.0 g, 23 mmol) was added portion wise to the cold solution. Iodomethane (1.2 mL, 20.0-mmol) was then added dropwise with stirring and the reaction was allowed to continue at 0 °C for 5 h. The reaction mixture was poured in ice-water (80 mL) and extracted with ether (2×100 mL). Combined organic layer was washed with water followed by brine and dried over anhydrous sodium sulphate. Evaporation of ether gave the solid mass of **2** which was chromatographed over silica gel (15 g) column using a mixture of *n*-hexane and dichloromethane (1:2) as eluent to afford the pure compound. It was then crystallised from dichloromethane-hexane.

6,7-dimethoxy-9-methyl-2,3,4,9-tetrahydro-1H-carbazol-1-one (DMTCO)

Solid; m.p.233 °C; IR (KBr): 2943, 1647,1590, 1511 cm–1; ^{1}H NMR (CDCl3, 500 MHz): δ 2.22 (quintet, 2 H, C3 –H), 2.61 (t, 2 H, C2 –H), 2.96 (t, 2 H, C4 –H), 3.92 (s, 3H, Ar-OCH_3), 3.94 (s, 3H, Ar-OCH_3), 4.02 (s, 3 H, N –CH3), 6.84 (s, 1 H, C_8–H), 6.92 (s, 1H, C_5–H); ^{13}C NMR (CDCl3, 125 MHz): δ 21.78(−), 25.14(−), 32.17(+), 37.98(−),56.28(+),56.28(+), 95.20(+), 101.12(+), 118.85(−), 129.72(−), 130.58(−), 133.92(−), 146.39(−), 152.16(−), 186.20(−); HRMS *m/z* Calcd for $C_{15}H_{18}NO_3$ [M+H]+260.1286, Found 260.1284.

5-methyl-8,9-dihydro-5H-[1,3]dioxolo[4,5-b]carbazol-6(7H)-one (MDDCO)

Solid; m.p.285 °C; IR (KBr): 2933, 1628,1574, 1501 cm–1; ^{1}H NMR (CDCl3, 500 MHz): δ 2.10 (quintet, 2 H, C3 –H), 2.47 (t, 2 H, C2 –H), 2.88 (t, 2 H, C4 –H), 4.04 (s, 3 H, N –CH3), 6.04 (s, 2H, Ar-OCH_2O-), 6.82 (s, 1 H, C_8–H), 6.98 (s, 1H, C_5–H);

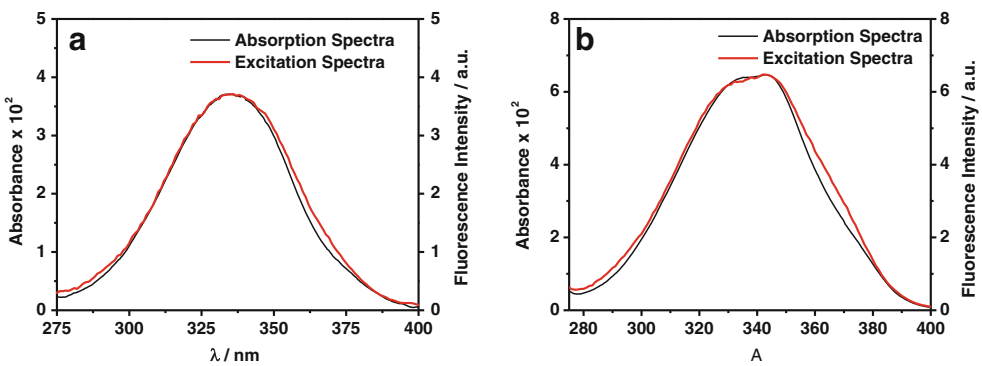

Fig. 6 Comparison of absorption and normalized fluorescence excitation spectra of (a) DMTCO and (b) MDDCO in ethanol

Table 4 $f_{LM}(\varepsilon, n)$ values of the solvents

Solvents	$f_{LM}(\varepsilon, n)$
BZ	0.0035
DOX	0.0213
THF	0.2109
ACN	0.3062
DMSO	0.2641
ETOH	0.2868
MEOH	0.3094
Tol	0.0141
EtAc	0.2005
DMF	0.2755
Water	0.3204
BuOH	0.2635
HxOH	0.2444
OcOH	0.2256
DcOH	0.2052
DdOH	0.1437

^{13}C NMR (CDCl3, 125 MHz): δ 21.48(−), 25.16(−), 32.24(+), 38.18(−),92.67(+),98.88(+), 101.04(−), 119.64(−), 128.85(−), 130.82(−), 134.78(−), 143.92(−), 148.39(−),189.20(−); HRMS *m/z* Calcd for $C_{14}H_{14}NO_3$ [M+H]+244.0973, Found 244.0974.

Results and Discussion

Photophysical Properties of DMTCO and MDDCO in Pure Solvents

DMTCO and MDDCO are Potential Fluorophores

UV–vis absorption spectra of both the compounds DMTCO and MDDCO have been monitored in sixteen different protic and aprotic solvents. The absorption maxima of the compounds appear within 320–350 nm (Fig. 3). Upon excitation at their respective absorption maxima in different solvents, DMTCO and MDDCO emit fluorescence with large stokes shifts (Fig. 4). The absorption and fluorescence emission maxima of the fluorophores have been listed in Table 2. Fluorescence quantum yields of the compounds have been calculated with anthracene as the reference fluorophore (Table 3). Standard procedure [1] has been followed for quantum yield calculation.

DMTCO and MDDCO Retain Their Ground State Structures in Electronic Excited State

Fluorescence excitation spectra of DMTCO and MDDCO have been measured in all the sixteen solvents with respect to their corresponding emission maxima (Fig. 5). In every case, the profiles of the absorption spectra and the fluorescence excitation spectra of both the compounds are similar (Fig. 6). Such observation indicates similarity in electronic distribution of DMTCO and MDDCO in ground and singlet excited states.

Enhancement of Dipole Moment in Excited State

Comparison of the absorption and emission spectra of the compounds in different solvents reveals that both DMTCO and MDDCO are less sensitive to solvent perturbation in electronic ground state compared to excited state (Figs. 3 & 4). The fluorescence emission maximum of the two probes has shifted steadily towards red when solvents with higher polarity and H-bonding ability have been used. These are indicative of more complete relaxation of the electronic excited state of the compounds in those solvents and can happen if the excited state dipole moment of the compounds is quite different than the corresponding ground state dipole moment. Specific interaction in the excited state of the compound like intermolecular hydrogen bonding can also play a vital role in such wavelength shifts because both the compounds contain heteroatoms that are potential sites for the formation of hydrogen bonds.

Solvatochromic shifts in fluorescence spectra can be explained based on the Onsager description of non-specific electrostatic solute–solvent interactions. For spherical solute molecules centred in a closed spherical first solvation shell, the solvent spectral shift is given by the following relation:

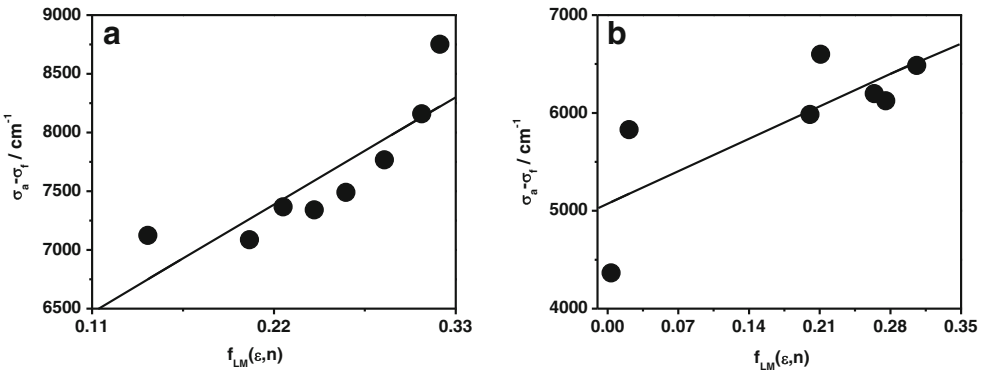

Fig. 7 Plot of σ_a–σ_f versus $f_{LM}(\varepsilon,n)$ in **a** aprotic and **b** protic solvents for DMTCO

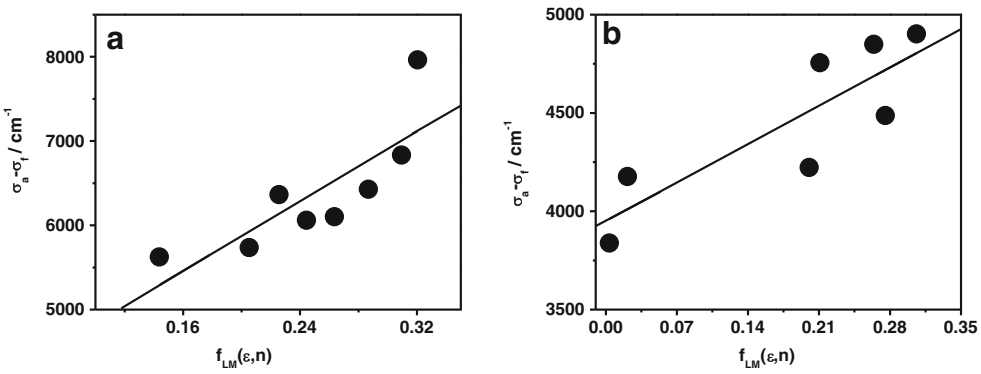

Fig. 8 Plot of σ_a–σ_f versus $f_{LM}(\varepsilon,n)$ in **a** aprotic and **b** protic solvents for MDDCO

$$\sigma_a - \sigma_f = mf(\varepsilon, n) + const \tag{1}$$

where,

$$m = \frac{2\left(\mu_e - \mu_g\right)^2}{hca^3} \tag{2}$$

Here, σ_a and σ_f are the wave numbers of the absorption and emission maxima respectively; μ_g and μ_e are the dipole moments in the ground and excited states; h is Planck's constant; c is the velocity of light in vacuum. For a spherical cavity with an Onsager radius a, the solvent polarity function is given by the following relation [19],

$$f(\varepsilon, n) = \frac{\frac{\varepsilon-1}{2\varepsilon+1} - \frac{n^2-1}{2n^2+1}}{\left(1 - \frac{2\alpha}{a^3} \cdot \frac{\varepsilon-1}{2\varepsilon+1}\right)\left(1 - \frac{2\alpha}{a^3} \cdot \frac{n^2-1}{2n^2+1}\right)^2} \tag{3}$$

where ε and n denote respectively the electric permittivity and refractive index of the solvents. α is the average polarizability ($\alpha_e \approx \alpha_g = \alpha$) of the solute.

In the theory proposed by Lippert [20] and Mataga [21], the polarizability of the solute is neglected ($\alpha = 0$) and so Eq. (3) is simplified to the following relation.

$$f_{LM}(\varepsilon, n) = \frac{\varepsilon-1}{2\varepsilon+1} - \frac{n^2-1}{2n^2+1} \tag{4}$$

For a special case where the ground and excited-state dipole moments (μ_g and μ_e) are parallel, the relation (3) yields the dipole moment difference $\Delta\mu$:

Table 5 Dipole moment change in the excited state of DMTCO and MDDCO in protic and aprotic solvents calculated using Lippert-Mataga method

Compounds	Protic Solvent	Aprotic Solvent
DMTCO	7.27 D	5.48 D
MDDCO	8.09 D	4.20 D

$$\Delta\mu = \left(\mu_e - \mu_g\right) = \left(\frac{1}{2} hca^3 . m\right)^{\frac{1}{2}} \tag{5}$$

$f_{LM}(\varepsilon,n)$ has been calculated for all the solvents used in this study (Table 4) and σ_a–σ_f vs. $f(\varepsilon,n)$ has been plotted for DMTCO and MDDCO in different protic and aprotic solvents (Figs. 7 and 8). The value of m has been obtained from the slopes of the plots in accordance with Eq. 1. Then Eq. (5) has been used to calculate the changes in dipole moments of DMTCO and MDDCO in protic and aprotic solvents (Table 5).

Disparity in Behaviour of Excited DMTCO and MDDCO in Protic and Aprotic Solvents

It has been observed that the fluorescence emission maxima of DMTCO and MDDCO shift bathochromically with solvent polarity. However, the extent and trend of the solvatochromic shifts of both fluorophores differ in protic and aprotic solvents. Dipole moment change in the excited state of the compounds is higher in protic solvents (Table 5) than in aprotic solvents. Moreover, in case of protic solvents, the fluorescence emission maxima of the compounds correlate linearly with the empirical parameters of the solvent, i.e., empirical polarity parameters $E_T(30)$ (Fig. 9), H-bond donor acidity α (Fig. 10), H-bond acceptor basicity β (Fig. 11) and polarizability π^* (Fig. 12). However, in aprotic solvents such correlations for the compounds are relatively poor (not shown). Such differences in the photophysical behaviour of both DMTCO and MDDCO in protic and aprotic solvents may originate from special type of probe-solvent interaction whose nature has been identified later in this work as intermolecular H-bonding.

Dependence of Solvatochromic Shifts of DMTCO and MDDCO on Empirical Parameters of Solvents

Kamlet-Taft Solvatochromic Comparison method (KTSCM) has been used to quantify the individual contributions of the polarity/polarizability effects of the solvent (π^*), its HBD

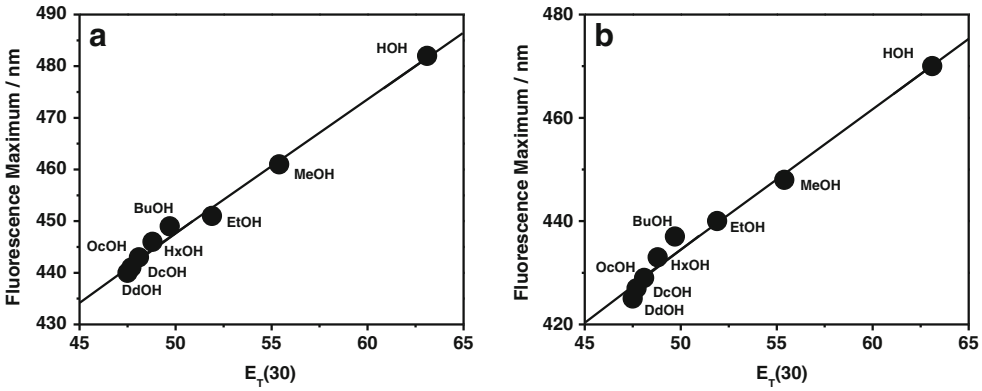

Fig. 9 Correlation of the fluorescence maxima of **a** DMTCO and **b** MDDCO with the empirical polarity parameters $E_T(30)$ of the protic solvents

(hydrogen bond donor) acidity (α) and its HBA (hydrogen bond acceptor) basicity (β) on the emission maxima of DMTCO and MDDCO. According to this method, wave numbers of the emission maxima of a fluorophore can be correlated with the empirical solvent parameters using the following multiple linear regression analysis approach [22–28].

$$\sigma = \sigma + s\pi^* + a\alpha + b\beta \tag{6}$$

Here, the coefficients s, a and b measure the relative sensitivities of the fluorophore to the said solvent properties. σ is the wave number of the emission maxima of the reference solvent.

Using the values of emission maxima of the compounds from Table 2 and the values of the solvent parameters from Table 1, following values are obtained for DMTCO (Eq. 7) and MDDCO (Eq. 8) using benzene as the reference solvent.

$$\sigma = 24876 - 1059\pi^* - 2667\alpha - 591\beta \tag{7}$$

$$\sigma = 25316 - 1243\pi^* - 2562\alpha - 345\beta \tag{8}$$

Emission frequencies have been expressed in cm^{-1}. The relative magnitudes of s, a and b indicate that HBD acidity of the solvent plays a major role on the photophysics of DMTCO and MDDCO while HBA basicity of the solvent plays a minor role. Solvent polarity/polarizability is found to be half significant as the HBD acidity of the solvent in controlling the emission behaviour of the compounds.

Ability to Distinguish Between the Hydrophobic and Hydrophilic Parts of Longer Chain Alcohols

The fluorescence decay profiles of DMTCO and MDDCO in different solvents have been shown in Fig. 13. The corresponding decay parameters have been calculated[1] using Eq. 9 and is listed in Table 6.

$$I(t) = \sum_{i=1}^{n} a_i e_i^{-t/\tau_i} \tag{9}$$

where I(t) is the intensity of the fluorescence at time t, a_i is the pre-exponential factor for the fraction of the fluorescence intensity, τ_i is the fluorescence lifetime of the emitting species and n is the total number of emitting species.

As shown in table 3, in all aprotic solvents as well as in some protic solvents viz. water, methanol and ethanol, the fluorescence lifetime decays of DMTCO and MDDCO has been fitted in single exponential decay equation. In the contrary, fluorescence decay profiles of the compounds in longer chain alcoholic solvents from butanol to dodecanol are better fitted in bi-exponential decay equation. The longer lifetime

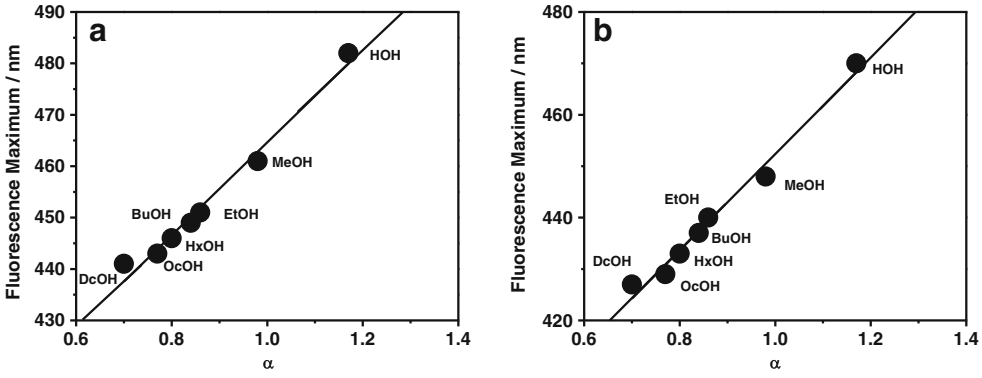

Fig. 10 Correlation of the fluorescence maxima of **a** DMTCO and **b** MDDCO with the H-bond donor acidity α of the protic solvents

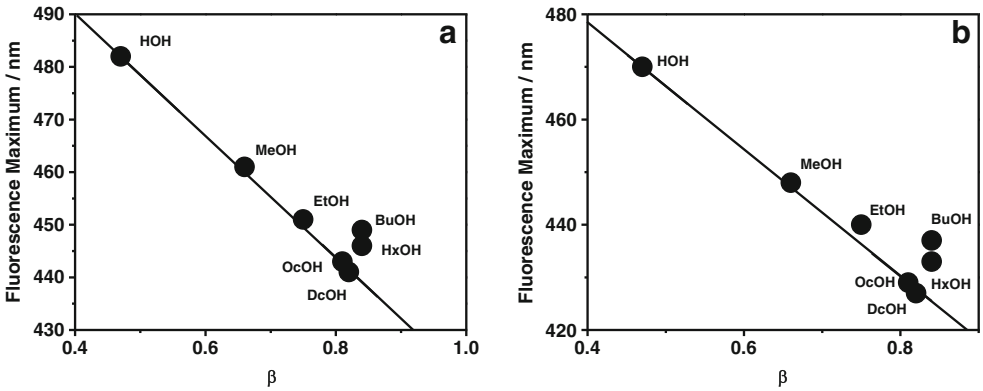

Fig. 11 Correlation of the fluorescence maxima of **a** DMTCO and **b** MDDCO with the H-bond acceptor basicity β of the protic solvents

component is similar in magnitude with protic solvents while the shorter lifetime component is similar in magnitude with less polar solvents (Table 6). Such observations, although unusual, can be explained based on the differential solvation of the probe molecules near the polar head groups and in the hydrophobic tail regions of such alcohols. Since the FWHM of the laser pulse used in experiment is 0.3 ns, and the lifetime of one of the components is below or very close to the 0.3 ns, the individual components residing in different zones of long chain alcohols cannot be resolved. The lifetimes in less polar aprotic solvents are approximately measured for similar reasons.

Relevance of H-bonding is significant from the fluorescence lifetimes of the compounds. HBD acidity decreases with the alcohol chain length from water to butanol and so the lifetime increases in the same order. Alcohols from butanol to decanol have similar average lifetime because all have similar HBD acidity and HBA basicity (Table 1). Among aprotic solvents, the lifetime is mainly dependant on the polarizability factor because these solvents have minimal or no HBD acidity and the contribution of HBA basicity is negligible on the emission of the fluorophores (section 3.1.6).

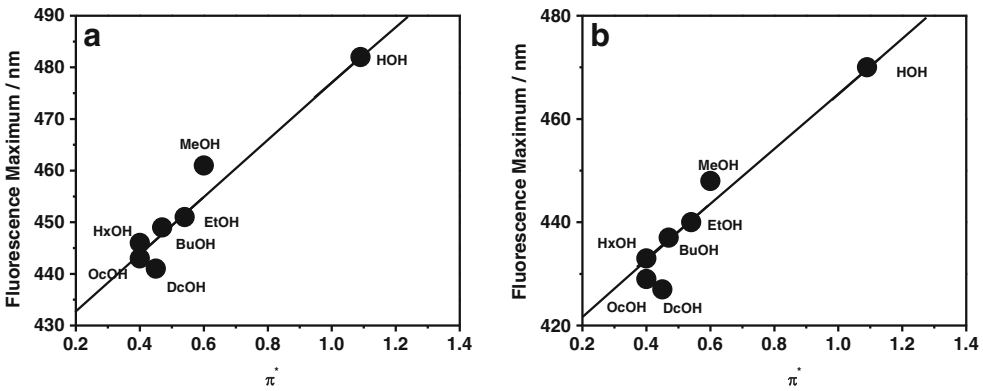

Fig. 12 Correlation of the fluorescence maxima of **a** DMTCO and **b** MDDCO with the polarizability π^* of the protic solvents

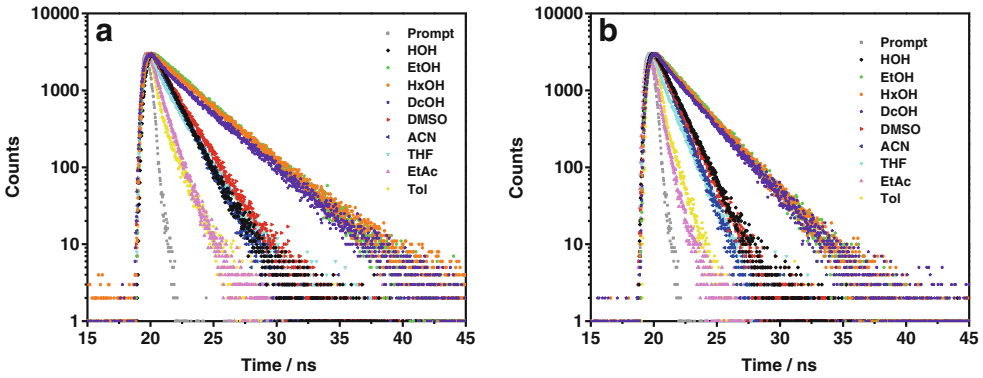

Fig. 13 Fluorescence lifetime decays of **a** DMTCO and **b** MDDCO in nine different solvents. The samples have been excited with 340 nm pulsed LED

Table 6 Fluorescence decay parameters of DMTCO and MDDCO [10^{-5} M] in sixteen different solvents.

Solvent	DMTCO				MDDCO			
	a_1 (a_2)	τ_1 (τ_2)	χ^2	τ	a_1 (a_2)	τ_1 (τ_2)	s^2	τ
HOH	1	1.318	0.999	1.318	1	1.255	1.010	1.255
MeOH	1	2.757	1.000	2.757	1	2.314	1.006	2.314
EtOH	1	3.015	0.999	3.015	1	2.332	1.000	2.332
BuOH	0.055 (0.945)	1.392 (3.130)	0.999	3.086	1	2.366	1.008	2.366
HxOH	0.051 (0.948)	0.257 (3.092)	1.000	3.080	0.032 (0.968)	0.288 (2.373)	1.100	2.365
OcOH	0.084 (0.916)	0.491 (3.127)	1.000	3.089	0.070 (0.930)	0.324 (2.345)	1.000	2.345
DcOH	0.107 (0.893)	0.706 (3.096)	0.998	3.033	0.094 (0.906)	0.471 (2.324)	1.000	2.286
DdOH	0.149 (0.851)	0.949 (3.087)	1.000	2.977	0.120 (0.880)	0.625 (2.309)	0.999	2.249
Bz	1	0.212	1.000	0.212	1	0.180	1.009	0.180
Tol	1	0.194	1.000	0.194	1	0.198	0.993	0.198
DOX	1	0.271	1.002	0.271	1	0.160	0.992	0.160
EtAc	1	0.248	1.001	0.248	1	0.495	1.000	0.495
THF	1	0.544	1.001	0.544	1	0.190	1.007	0.190
ACN	1	1.374	1.000	1.374	1	1.015	1.000	1.015
DMF	1	1.306	0.999	1.305	1	0.856	1.005	0.856
DMSO	1	1.618	1.001	1.618	1	1.206	1.009	1.206

Additional Pathways of DMTCO and MDDCO for Deexcitation in Less Polar Solvents

The radiative (k_r) and non-radiative (k_{nr}) decay rates of the compounds in different solvents have been calculated[1] using relations 10 and 11 and listed in table 7.

$$k_r = \frac{\phi_f}{\tau_f} \tag{10}$$

$$k_{nr} = \frac{(1-\phi_f)}{\tau_f} \tag{11}$$

Here, ϕ_f and τ_f are the fluorescence quantum yields and fluorescence lifetimes of the probes in a particular medium. For bi-exponential decays, average lifetimes have been used to calculate the radiative and non-radiative decay rates.

The increase in the non-radiative decay rates from more polar to less polar aprotic solvents (Fig. 14) indicates that in non-polar aprotic solvents additional pathways for deactivation of excited singlet state become pronounced compared to those in polar solvents. This is possibly the intersystem crossing (ISC) since both DMTCO and MDDCO have transient absorption. For protic solvents, maximum of non-radiative decay rate is found in solvents of intermediate polarity and unlike aprotic solvents, water, which is the most polar, has maximum non-radiative decay rate. Such a trend can be explained considering the better collision induced vibrational relaxation (CIVR) in more intramolecularly H-bonded water.

Photophysical Properties of DMTCO and MDDCO in Binary Solvent Mixtures

Similar Behaviour of DMTCO and MDDCO in Pure Solvents and Binary Solvent Mixtures with Similar Polarity

A well characterized [29–31] water-1,4-dioxane mixture system has been chosen to compare the photophysical response

Table 7 Radiative (k_r) and non-radiative (k_{nr}) decay rates of (a) DMTCO and (b) MDDCO [10^{-5} M] in different solvents

Solvents	DMTCO		MDDCO	
	$k_r \times 10^{-7}/s^{-1}$	$k_{nr} \times 10^{-7}/s^{-1}$	$k_r \times 10^{-7}/s^{-1}$	$k_{nr} \times 10^{-7}/s^{-1}$
HOH	2.597	73.281	5.989	73.692
MeOH	4.481	31.785	9.290	33.919
EtOH	3.920	29.247	10.079	32.796
BuOH	5.079	27.322	10.679	31.594
HxOH	4.657	27.814	13.263	29.020
OcOH	5.093	27.278	12.300	30.349
DcOH	4.742	28.231	10.612	33.138
DdOH	1.285	32.300	0.282	44.188
Bz	16.887	455.256	21.419	535.064
Tol	16.211	499.785	10.403	493.883
DOX	16.572	352.977	32.537	590.904
EtAc	19.414	384.463	8.937	192.961
THF	15.469	168.489	46.732	478.203
ACN	9.405	63.364	13.841	84.632
DMF	9.453	67.152	16.599	100.156
DMSO	9.259	52.534	16.511	66.415

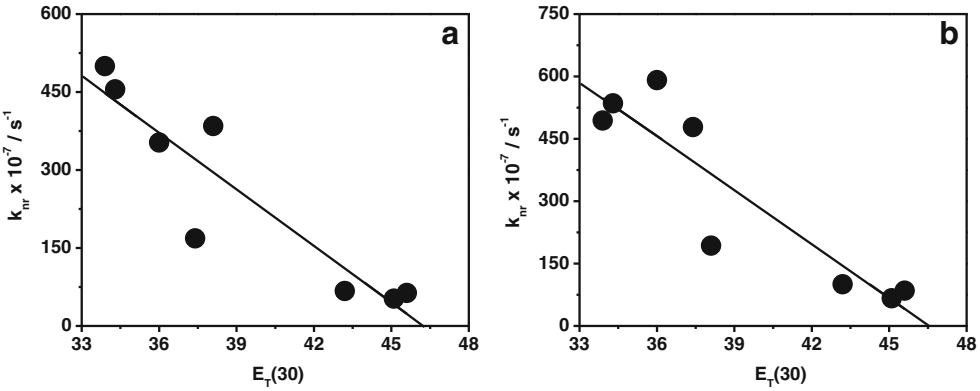

Fig. 14 Variation of non-radiative decay rates (k_{nr}) of **a** DMTCO and **b** MDDCO vs empirical polarity parameter of aprotic solvents

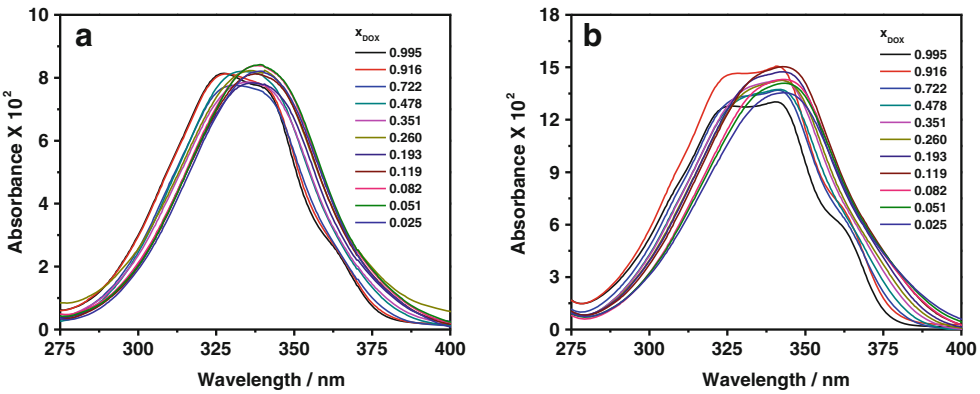

Fig. 15 Absorption spectra of **a** DMTCO and **b** MDDCO [2.5×10^{-6} M] in different mole fraction of 1,4-dioxane (x_{DOX}) in water-1,4-dioxane solvent mixtures

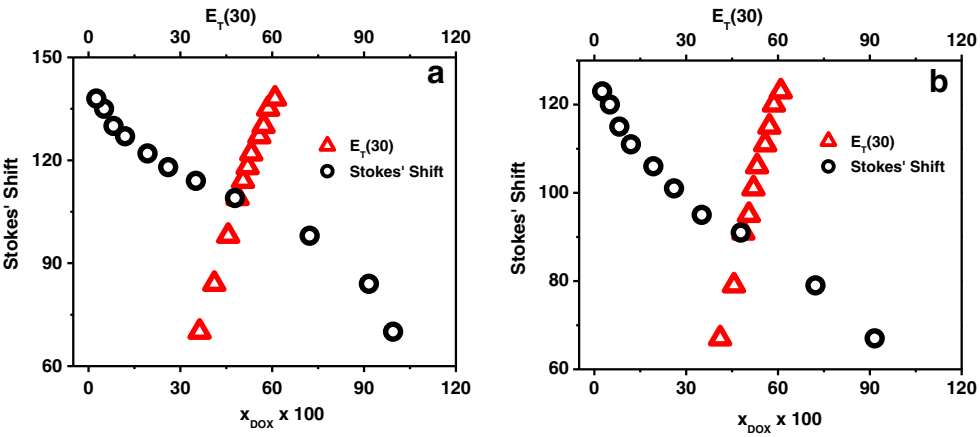

Fig 16 Dependence of Stokes shift of **a** DMTCO and **b** MDDCO [2.5×10^{-6} M] on the mole fraction of 1,4-dioxane (x_{DOX}) in water-1,4-dioxane solvent mixtures and on the values of empirical polarity parameters, E_T(30) of the solvent mixtures

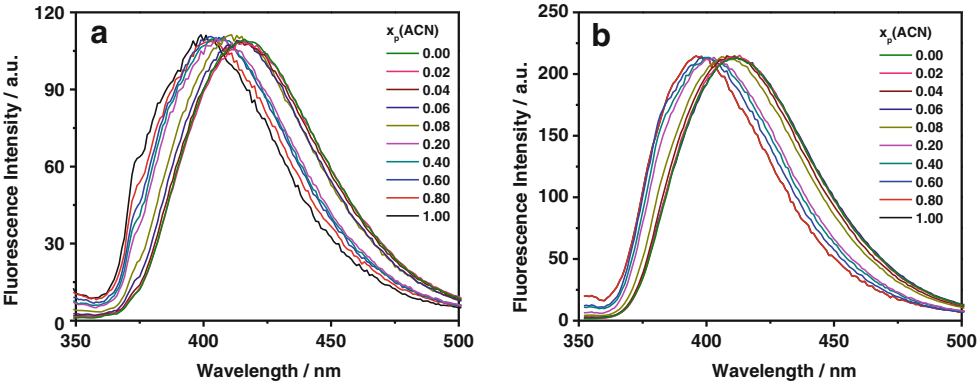

Fig. 17 Steady-state fluorescence spectra of **a** DMTCO and **b** MDDCO in toluene-acetonitrile solvent mixtures with different mole fraction of acetonitrile (x_p)

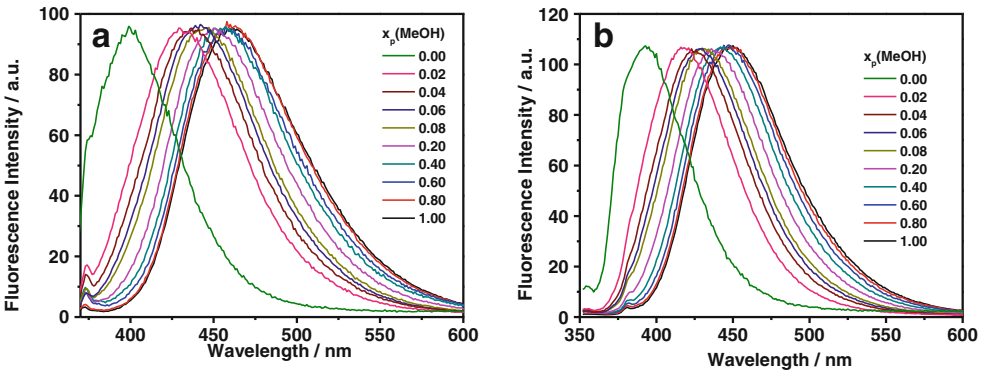

Fig. 18 Steady-state fluorescence spectra of **a** DMTCO and **b** MDDCO in toluene-methanol solvent mixtures with different mole fraction of methanol (x_p)

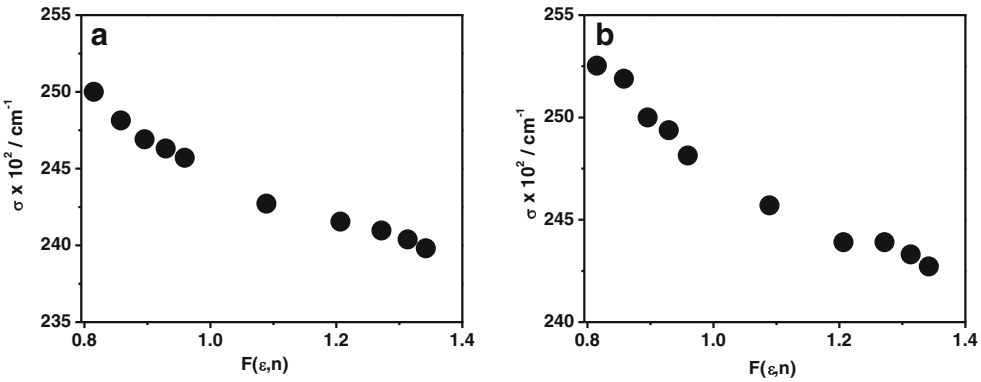

Fig. 19 Plot of the wave number (σ) of fluorescence emission maxima of **a** DMTCO and **b** MDDCO as a function of the reaction field factor $F(\varepsilon, n)$ in toluene-acetonitrile solvent mixtures

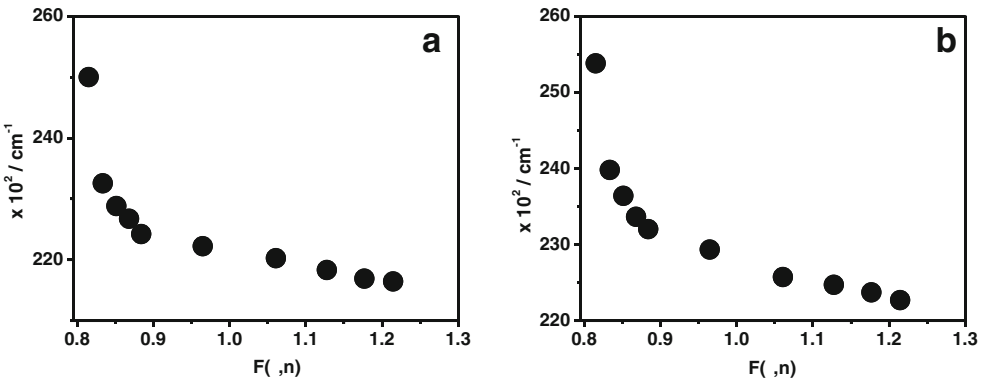

Fig. 20 Plot of the wave number (σ) of fluorescence emission maxima of **a** DMTCO and **b** MDDCO as a function of the reaction field factor $F(\varepsilon, n)$ in toluene-methanol solvent mixtures

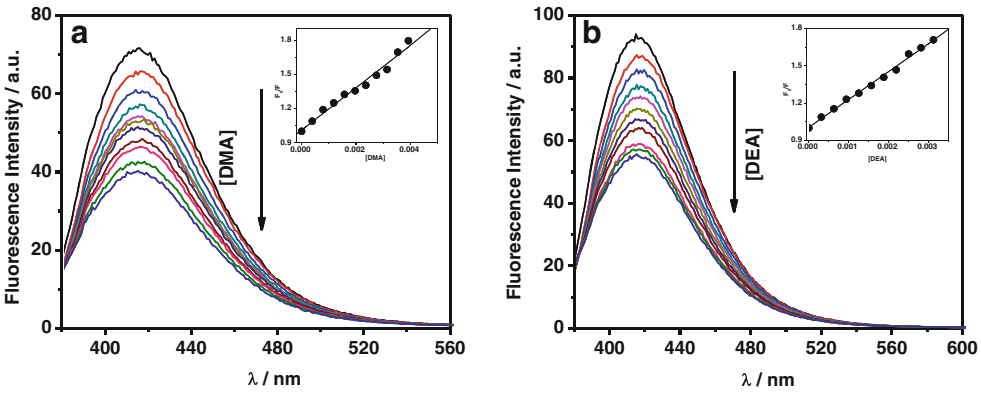

Fig. 21 Fluorescence quenching of DMTCO with **a** DMA and **b** DEA in acetonitrile medium. Concentration of the DMTCO is 1×10^{-6} M during the experiment

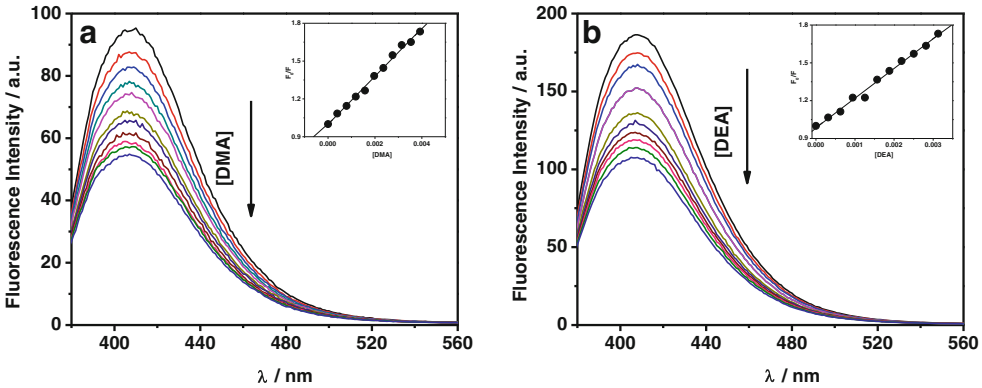

Fig. 22 Fluorescence quenching of MDDCO with **a** DMA and **b** DEA in acetonitrile medium. Concentration of the MDDCO is 1×10^{-6} M during the experiment

of the compounds in pure solvents and in binary solvent mixtures. Similar to that in pure solvents, absorption maxima of DMTCO and MDDCO shifts to a small extent at different compositions of the solvent mixtures (Fig. 15). Moreover, the fluorescence emission maxima shift bathochromically when the mole fraction of the protic component, i.e. water, is increased and correspondingly the empirical polarity [$E_T(30)$] of the solvent mixture is increased [32]. Figure 16 displays pictorially the dependence of the stokes shifts of the fluorescence emission maxima on the mole fraction of 1,4-dioxane and the empirical polarity parameters at each composition. These two observations indicate that the compounds behave identically in pure solvents and binary solvent mixtures.

Excited State Intermolecular H-bonding of DMTCO and MDDCO with Protic Solvents

Since there is a close resemblance in the behaviour of the compounds in pure solvents and in binary solvent mixtures, an attempt has been made to compare the photophysical response of DMTCO and MDDCO in two different solvent mixtures toluene-acetonitrile and toluene-methanol. The uniqueness of these solvent mixtures is that the polar components acetonitrile and methanol have similar dielectric constants and refractive indices (Table 1), but methanol can form hydrogen bonds while acetonitrile cannot. Such solvent mixture systems are used to demonstrate the hydrogen bond forming ability of compounds [33–35].

Table 8 Stern-Volmer quenching constants of DMTCO and MDDCO with DMA & DEA in acetonitrile medium

Quenching Constants, $[M]^{-1}$	DMTCO	MDDCO
DMA	185.5	190.5
DEA	223.3	235.5

Fluorescence maxima of DMTCO and MDDCO shift towards red when fraction of the polar component increases in either toluene-acetonitrile or toluene-methanol solvent mixtures [Figs. 17 and 18].

Difference in the behaviour of the compounds in these two solvent mixtures is that the fluorescence maxima of DMTCO and MDDCO in toluene-methanol solvent mixtures are not a linear function of methanol concentration. On the contrary, in toluene-acetonitrile solvent mixtures, the red shift occurs almost linearly with increase in acetonitrile concentration. This has been shown pictorially in Figs. 19 and 20 with the variation of fluorescence maxima of DMTCO and MDDCO as a function of the reaction field factor at each composition which according to dielectric continuum theory is the best measure of solvation energy and solvatochromic shifts [33–35].

The dielectric continuum theory predicts that solvatochromic shifts of the fluorescence spectra for a molecule in solvents of different polarity should be proportional to the reaction field factor. Reaction field factor $F(\varepsilon,n)$, often used as a measure of solvation energy is related to the dielectric constant (ε) and refractive index (n) of a medium.

$$F(\varepsilon,n)=\frac{\varepsilon-1}{\varepsilon+2}-\frac{n^2-1}{n^2+2} \tag{12}$$

Dielectric constant (ε) and refractive index (n) of toluene-acetonitrile and toluene-methanol solvent mixtures have been calculated using the previously reported empirical equations.

For toluene-acetonitrile solvent mixtures,

$$n=1.495-0.084x_p+0.003{x_p}^2-0.072{x_p}^3 \tag{13}$$

$$\varepsilon=2.38+14.6x_p-4.16{x_p}^2+22.9{x_p}^3 \tag{14}$$

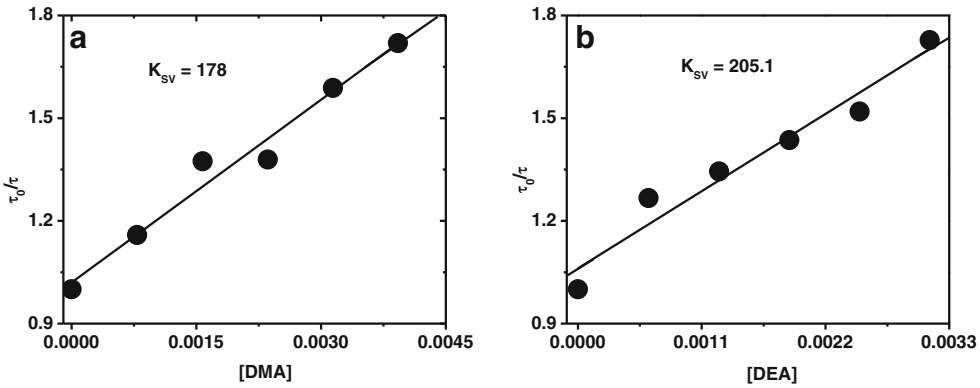

Fig. 23 Fluorescence lifetime quenching plots of DMTCO with **a** DMA and **b** DEA in acetonitrile medium. Concentration of the DMTCO is 1×10^{-6} M during the experiment

For toluene-methanol solvent mixtures,

$$n = 1.495 - 0.063x_p + 0.014{x_p}^2 - 0.117{x_p}^3 \quad (15)$$

$$\varepsilon = 2.38 + 6.13x_p - 0.14{x_p}^2 + 24.03{x_p}^3 \quad (16)$$

Here, x_p is the mole fraction of the polar component in the solvent mixture.

Such observation indicates that in toluene-acetonitrile solvent mixtures, there is no dielectric enrichment for the excited state of the molecules. Dielectric enrichment of electronically excited DMTCO and MDDCO in toluene-methanol solvent mixture clearly indicates a special interaction of the compounds with methanol most likely originating from intermolecular hydrogen bonding.

Interaction of DMTCO and MDDCO with Organic Bases

Dynamic Fluorescence Quenching of the Compounds in Presence of Organic Electron Donors

It has been observed that the fluorescence of DMTCO and MDDCO is quenched in the presence of some organic electron donors, N,N-dimethylaniline (DMA) and N,N-diethylaniline (DEA). No changes in the absorption spectra of both the compounds in acetonitrile (not shown) have been observed even after addition of high concentration of these bases indicates that the interactions occur only in the electronic excited state. The quenching constants in acetonitrile have been measured using Stern-Volmer relation [1].

$$\frac{F_o}{F} = 1 + K_{sv}[Q] \quad (17)$$

In Eq. (17) F_0 and F are the relative fluorescence intensities in the absence and presence of the quencher (Q) and K_{sv} is the Stern-Volmer quenching constant.

These Stern-Volmer quenching constant values have been calculated from the Figs. 21 and 22 and are listed in table 8.

Similar quenching has been found with fluorescence lifetimes [Fig. 23], which indicates that the nature of quenching is dynamic in nature.

DMTCO and MDDCO act as an Electron Acceptor in Excited State

Excited state interaction between the compounds and organic bases may be due collisional quenching, energy transfer or electron transfer. Occurrence of energy transfer can be ruled out since there is no overlap of the fluorescence spectra of the compounds with the absorption spectra of the organic amines. Simple collisional quenching can also be ruled out considering the quenching rate constants (~ 10^{11} s^{-1}). From structural point of view, DEA is a better electron donor (base) than DMA. MDDCO is enriched with the A ring than the DMTCO molecule (Scheme 2) that can add the extra rigidity and impart higher extent of planarity of the MDDCO molecule. This implies higher electron accepting capability of MDDCO than that of DMTCO as extent of electronic delocalisation is lower in the latter case.

Since the trend in the value of quenching constant (Table 8) matches with the basicity of the amines and the acceptor ability of the compounds, electron transfer is the most probable mechanism of this excited state interaction. This assertion has further been verified using Laser Flash Photolysis experiments. With such experiments one can identify the presence of transient reactive intermediates in an electron transfer reaction [16, 36–39]. For a photoinduced

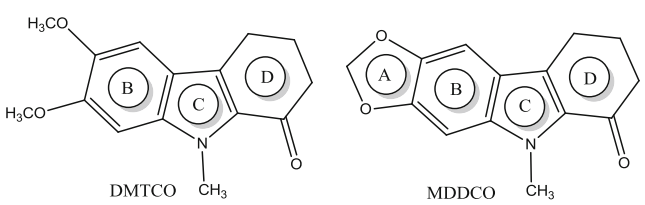

Scheme 2 Structural variations of DMTCO and MDDCO

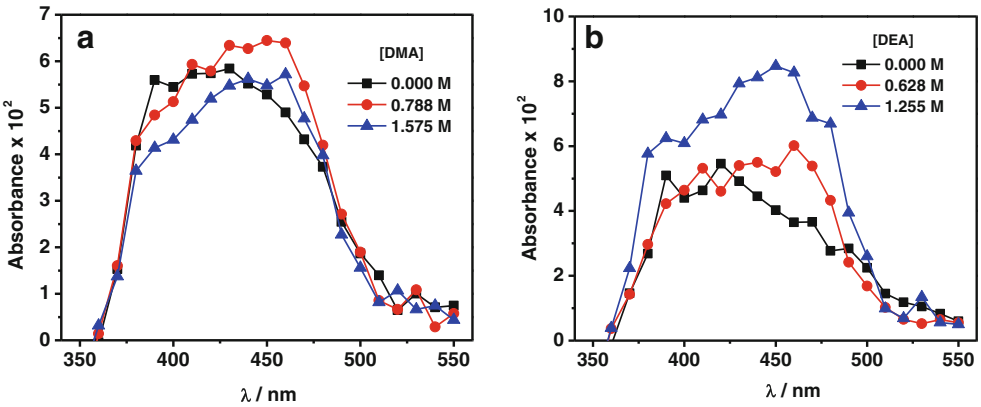

Fig. 24 Transient absorption spectra of DMTCO at 0.5 μs time delay with varying concentrations of **a** DMA and **b** DEA. Concentration of DMTCO was kept at 10^{-4} M during the experiment

electron transfer from DMA and DEA to the compounds, radical cations of the amines (DMA● + and DEA●+) should form along with the radical anions of DMTCO and MDDCO (DMTCO●- and MDDCO●-).

DMTCO + DMA → DMTCO●- + DMA●+
DMTCO + DEA → DMTCO●- + DEA●+
MDDCO + DMA → MDDCO●- + DMA●+
MDDCO + DEA → MDDCO●- + DEA●+

As shown in Figs. 24 and 25, the transient absorption spectra of DMTCO and MDDCO have hump around 400 to 450 nm. On addition of the amines, the transient absorption spectrum of the compounds quenches, with the relative increase in transient absorption around 470 nm which could be due the radical cations of DMA or DEA [40]. The absorbance due to the radical anions is expected to have merged with the absorbances of radical cations and compounds. Based on such observations, it can be conclusively stated that photoinduced electron transfer (PET) from the organic amine electron donors to the compounds DMTCO and MDDCO is the reason of such excited state interaction.

Conclusions

Two fluorophores, DMTCO and MDDCO have been synthesized and their optical response have been studied in pure solvents as well as binary solvent mixtures. Comparison of absorption spectra and fluorescence excitation spectra of the compounds indicate that their structural integrity remains intact in the electronic excited state. Absorption maxima of DMTCO and MDDCO shifts to a small extent on changing the solvent or varying the composition of the binary solvent mixtures. On contrary, the fluorescence emission maxima of the compounds are largely dependent on the nature of the solvent or the composition of the solvent mixture. The fluorophores behave in a more regular fashion in protic solvents which is evident from the plots of emission maxima versus empirical solvent parameters. Moreover DMTCO and MDDCO show better sensitivity towards protic solvents and as a consequence dipole moment change of the compounds in the excited state of the compounds is higher in protic solvents. Excited state photophysics of both the compounds is dependent mostly on the HBD acidity of the solvent and also on solvent polarizability. HBA basicity of the solvent have minimal influence of the fluorescence emission of the compounds. Bi-exponential decay of both the compounds in

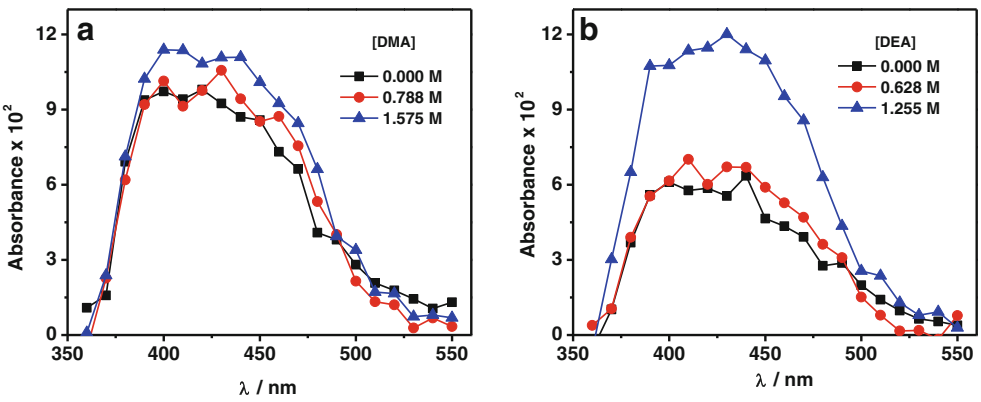

Fig. 25 Transient absorption spectra of MDDCO at 0.5 μs time delay with varying concentrations of **a** DMA and **b** DEA. Concentration of MDDCO was kept at 10^{-4} M during the experiment

higher chain alcohols is due to their differential solvation in polar head group and hydrophobic chains. Electronically excited DMTCO and MDDCO undergo dielectric enrichment in toluene-methanol solvent mixture but not in toluene-acetonitrile solvent mixture. Such observations indicate a special interaction of the compounds with protic solvent which possibly originates from intermolecular hydrogen bonding. Both the compounds DMTCO and MDDCO interact with organic bases DMA and DEA in the electronic excited state. Laser flash photolysis studies indicate that photoinduced electron transfer from the organic bases to the compounds is the reason of such interaction.

Acknowledgements We are thankful to Council of Scientific and Industrial Research (CSIR), New Delhi, India for providing research fellowships to two of the authors [Amrit Krishna Mitra: SRF, File No. 09/951(0003)/2009-EMR-I and Sujay Ghosh: SRF, File No. 09/489(0064)/2009-EMR-I]. This work has been funded by CBAUNP, MMDDA, BARD projects of SINP and DAE, CSIR projects of the Govt. of India. We are also thankful to Prof. Krishnangshu Roy, Director, School of Tropical Medicine, Kolkata and Prof. Milan Kumar Sanyal, Director, Saha Institute of Nuclear Physics, Kolkata for their interest in the work.

References

1. Lakowicz JR (2006) Principles of Fluorescence Spectroscopy. Springer, New York
2. Ranjith C, Vijayan KK, Praveen VK, Kumar NSS (2010) Photophysical investigation of 3-substituted 4-alkyl and/or 7-acetoxy coumarin derivatives—A study of the effect of substituents on fluorescence. Spectrochim Acta Part A 75:1610–1616
3. Pişkin M, Durmuş M, Bulut M (2012) Synthesis and investigation on photophysical and photochemical properties of 7-oxy-3-methyl-4-phenylcoumarin bearing zinc phthalocyanines. Spectrochim Acta Part A 97:502–511
4. Gaber M, El-Daly SA, Fayed TA, El-Sayed YS (2008) Photophysical properties, laser activity and photoreactivity of a heteroaryl chalcone: a model of solvatochromic fluorophore. Opt Las Tech 40:528–537
5. Bojinov VB, Panova IP, Grabchev IK (2007) Novel polymerizable light emitting dyes – combination of a hindered amine with a 9-phenylxanthene fluorophore. Synthesis and photophysical investigations. Dye Pigm 74:187–194
6. Feng J, Chen X, Han Q, Wang H, Lu P, Wang Y (2011) Naphthalene-based fluorophores: Synthesis characterization, and photophysical properties. J Lumin 131:2775–2783
7. Wang ZW, Cao QY, Lin S, Zhuo L, Li ZH (2013) 2,6-Diphenylpyridine-based fluorophores: Synthesis, photophysical properties and effects of protonation. J Photochem Photobiol A 251:106–112
8. Saito Y, Shinohara Y, Ishioroshi S, Suzuki A, Tanaka M, Saito I (2011) Synthesis of environmentally sensitive 2′-deoxyguanosine containing solvatochromic pyrene fluorophore. Tet Lett 52:2359–2361
9. Bag SS, Pradhan MK, Kundu R, Jana S (2013) Highly solvatochromic fluorescent naphthalimides: Design, synthesis, photophysical properties and fluorescence switch-on sensing of ct-DNA. BioMed Chem Lett 23:96–101
10. Ooyama HE, Ooyama Y, Hino T, Sakamoto T, Yamaguchi T, Yoshida K (2011) Synthesis and photophysical properties of structural isomers of novel 2,10-disubstituted benzofuro[2,3-e] naphthoxazole-type fluorescent dyes. Dye Pigm 91:481–488
11. Firmino ADG, Gonçalves MST (2012) Bifunctionalised long-wavelength fluorescent probes for biological applications. Tet Lett 53:4946–4950
12. Li Y, Scudiero L, Ren T, Dong WJ (2012) Synthesis and characterizations of benzothiadiazole-based fluorophores as potential wavelength-shifting materials. J Photochem Photobiol A 231:51–59
13. Dey D, Bose A, Bhattacharyya D, Basu S, Maity SS, Ghosh S (2007) Dibenzo[a, c]phenazine: A Polarity-Insensitive Hydrogen-Bonding Probe. J Phys Chem A 111:10500–10506
14. Knölker HJ, Reddy KR (2002) Isolation and synthesis of biologically active carbazole alkaloids. Chem Rev 102:4303–4428
15. Schmidt AW, Reddy KR, Knölker HJ (2012) Occurrence, biogenesis, and synthesis of biologically active carbazole alkaloids. Chem Rev 112:3193–3328
16. Mitra AK, Ghosh S, Chakraborty S, Sarangi MK, Saha C, Basu S (2012) Photophysical properties of an environment sensitive fluorophore 1-keto-6,7-dimethoxy-1,2,3,4-tetrahydrocarbazole and its excited state interaction with N, N-dimethylaniline: A spectroscopic investigation. J Photochem Photobiol A 240:66–74
17. Chakraborty S, Chattopadhyay G, Saha C (2011) Montmorillonite-KSF induced Fischer indole cyclization under microwave towards a facile entry to 1-keto-1,2,3,4-tetrahydrocarbazoles. Ind J Chem B 50:201–206
18. Mitra AK, Ghosh S, Chakraborty S, Basu S, Saha C Synthesis and Spectroscopic Exploration of Carboxylic Acid Derivatives of 6-Hydroxy-1-Keto-1,2,3,4-tetrahydrocarbazole: Hydrogen Bond Sensitive Fluorescent Probes. J Lumin accepted
19. Kawski A, Bojarski P, Kuklinski B (2008) Estimation of ground- and excited-state dipole moments of Nile red dye from solvatochromic effect on absorption and fluorescence spectra. Chem Phys Lett 463:410–412
20. Lippert E (1957) Spektroskopische bestimmung des dipolmomentes aromatischer Verbindungen im ersten angeregten singulettzustand. Ber Bunsenges Phys Chem 61:962–975
21. Mataga N, Kaifu Y, Koizumi M (1956) Solvent effects upon fluorescence spectra and the dipolemoments of excited molecules. Bull Chem Soc Jpn 29:465–470
22. Kamlet MJ, Abboud JLM, Abraham MH, Taft RW (1983) Linear solvation energy relationships. 23. A comprehensive collection of the solvatochromic parameters, pi.*, alpha., and.beta., and some methods for simplifying the generalized solvatochromic equation. J Org Chem 48:2877–2887
23. Abraham MH, Grellier PL, Abboud JLM, Doherty RM, Taft RW, Doherty M (1988) Solvent effects in organic chemistry — recent developments. Can J Chem 66:2673–2686
24. Kamlet MJ, Abboud JLM, Taft RW (1977) The solvatochromic comparison method. 6. The.pi.* scale of solvent polarities. J Am Chem Soc 99:6027–6038
25. Kamlet MJ, Taft RW (1976) The solvatochromic comparison method. I. The.beta.-scale of solvent hydrogen-bond acceptor (HBA) basicities. J Am Chem Soc 98:377–383
26. Taft RW, Abboud JLM, Kamlet MJ (1981) Solvatochromic comparison method. 20. Linear solvation energy relationships. 12. The d.delta. term in the solvatochromic equations. J Am Chem Soc 103:1080–1086
27. Taft RW, Kamlet MJ (1976) The solvatochromic comparison method. 2. The.alpha.-scale of solvent hydrogen-bond donor (HBD) acidities. J Am Chem Soc 98:2886–2894

28. Kamlet MJ, Dickinson C, Taft RW (1981) Linear solvation energy relationships Solvent effects on some fluorescence probes. Chem Phys Lett 77:69–72
29. Critchfield FE, Gibson JA, Hall JL (1953) Dielectric constant for the dioxane—water system from 20 to 35°. J Am Chem Soc 75:1991–1992
30. Geddes JA (1933) The fluidity of dioxane - water mixtures. J Am Chem Soc 55:4832–4837
31. Stallard RD, Amis ES (1952) Heat of vaporization and other properties of dioxane, water and their mixtures. J Am Chem Soc 74:1781–1790
32. Kosower EM, Dodiuk H, Tanizawa K, Ottolenghi M, Orbach N (1975) Intramolecular donor - acceptor systems. Radiative and nonradiative processes for the excited states of 2-N-arylamino-6-naphthalenesulfonates. J Am Chem Soc 97:2167–2178
33. Reynolds L, Gardecki JA, Frankland SJV, Horng ML, Maroncelli M (1996) Dipole Solvation in nondipolar solvents: experimental studies of reorganization energies and solvation dynamics. J Phys Chem 100:10337–10354
34. Suppan P (1990) Invited review solvatochromic shifts: the influence of the medium on the energy of electronic states. J Photochem Photobiol A 50:293–330
35. Kro´licki R, Jarzeba W, Mostafavi M, Lampre I (2002) J Phys Chem A 106:1708–1713
36. Tang R, Zhang P, Lia H, Liu Y, Wang W (2011) Photosensitized xanthone-based oxidation of guanine and its repair: a laser flash photolysis study. J Photochem Photobiol B 105:157–161
37. Li K, Wang H, Cheng L, Wang M, Zhua R, Wang SL (2011) Characterization of transient species produced from laser flash photolysis of a new cardioprotective drug: S-propargyl-cysteine. J Photochem Photobiol B 219:195–199
38. Rigoli IC, Bonilha JBS, Quina FH, Okano LT, Naal RMZG (2011) Photoreactions of n-alkyl-3-nitrophenyl ethers with aromatic amines in SDS micelles: a laser flash photolysis study. J Photochem Photobiol A 222:34–39
39. Sarangi MK, Basu S (2011) Associated electron and proton transfer between Acridine and Triethylamine in AOT reverse micelles probed by laser flash photolysis with magnetic field. Chem Phys Lett 506:205–210
40. Wang JT, Sun Q, Zhang LM, Yu SQ (2010) Solvent effects of photoinduced electron transfer reactions of triplet fluorenone with amines. Chin Sci Bull 55:2891–2895